Simulated Moving Bed under Linear Conditions: Experimental vs. Calculated Results

Tong Yun
Dept. of Chemical Engineering, University of Tennessee, Knoxville, TN 37996

Guoming Zhong and Georges Guiochon
Dept. of Chemistry, University of Tennessee, Knoxville, TN 37996

A simulated moving bed (SMB) was operated for the separation of mixtures of 2-phenyl ethanol and 3-phenyl-1-propanol on columns packed with Zorbax C18 bonded silica, using a 60:40 (v/v) solution of methanol and water as the mobile phase. Series of four or eight columns were used. The experiments were carried out with low concentration mixtures, that is, under linear conditions. Band profiles of both compounds eluted from one of the columns during successive periods after steady state had been reached were recorded, as were the concentration histories at the extract and raffinate ports. These experimental results are compared to those predicted by two models: the linear ideal and the linear equilibrium-dispersive models of chromatography, applied to the SMB separator. These two models give excellent agreement between the experimental profiles and those calculated with the model. As expected, the profiles predicted by the ideal and the equilibrium-dispersive models differ only by the lack of dispersion in the profiles given by the former. The latter model is demonstrated to be a solid, reliable tool for further studies of the SMB design and optimization.

Introduction

In spite of the progress made in contour procedures with the advent of computers, engineers still much prefer continuous processes over batch ones for industrial applications. Considerable effort has been made to replace the conventional methods of preparative chromatography by a continuous process. Overloaded elution under either isocratic or gradient conditions and displacement are batch processes. A feed pulse is injected in the unit and separated into its components, which are collected before a new batch can be processed. One of the major drawbacks of this approach is the finite recovery yield of the components of interest. Bands cannot be completely separated unless low production rates are accepted. The mixed fractions could be recycled, and serious consideration has been given to this approach by a few groups (Bailly and Tondeur, 1982; Bombaugh et al., 1969; Charton et al., 1994; Henry et al., 1974; Martin et al., 1976; Seidel-Morgenstern and Guiochon, 1993). However, it has proven difficult to find experimental conditions under which the production rate is equal to the one achieved in the conventional process (Charton et al., 1994; Seidel-Morgenstern and Guiochon, 1993). Because recycling is more complex and difficult to optimize, it has never received much attention from users. Simulated moving bed separators (SMB) now appear to be a much more attractive alternative to the batch processes.

SMB was invented by Broughton in 1961 as an alternative to countercurrent chromatography (Broughton and Gerhold, 1961; Broughton, 1968, 1978, 1984; de Rosset et al., 1970). In this last process, the solid phase is moved in the direction opposite to that of the liquid phase. The solid-phase velocity is selected so that the more retained components of the feed exit from each column in the direction of the solid phase, while the less retained ones exit in the direction of the liquid phase. Unfortunately, it has proven impossible to move the solid phase through the column and, at the time, achieve a reasonable column efficiency. SMB simulates the solid-phase movement by column switching. Thus, the solid phase moves by jumps that take place at an adjustable frequency. The proc-

Correspondence concerning this article should be addressed to G. Guiochon.
Additional address for T. Yun, G. Zhong, and G. Guiochon: Division of Analytical Chemistry, Oak Ridge National Laboratory, Oak Ridge, TN 37831.

ess is not really continuous, but periodic. As a consequence, its properties are somewhat different from those of true countercurrent chromatography (Ruthven and Ching, 1989). SMB has been applied to several important industrial separations, especially the extraction of *p*-xylene from C8 hydrocarbon fractions (Parex process (Broughton et al., 1970)) and that of fructose and glucose from hydrogenated corn syrup (Sarex process (Neuzil and Jensen, 1978)). SMB is now attracting considerable interest as a continuous process implementing preparative chromatography for industrial separations in the pharmaceutical industry. The most important field of application would be the separation of enantiomers, in which case the main inconvenience of the process, the impossibility of separating more than two components in a simple SMB, disappears. Compared to the classic applications of SMB in the chemical industry, however, applications in the pharmaceutical industry would be characterized by a much smaller specific capacity of the adsorbent, lower values of the separation factor, and the absolute need to work under nonlinear conditions.

So far most of the publications regarding SMB are devoted either to technical descriptions of some new applications (Negawa and Shoji, 1992; Ching et al., 1993; Küsters et al., 1995), or improvements made on the classic implementation of the process (Hashimoto et al., 1993; Balannec and Hotier, 1993; Charton and Nicoud, 1995), or to discussions of its modeling and interpretation. An important body of work is available in this last area, with pioneering work by Ruthven and Ching (1989) and important contributions of Storti et al. (1989, 1993), Fish et al. (1993), Yun et al. (1996), and Zhong and Guiochon (1996). However, few comparisons between the actual performance of the SMB and the predictions of the model have been published. Recently, Seidel-Morgenstern (1996) reported partial results comparing the concentration histories at the extract and raffinate ports during startup operation and showing good agreement with the calculated chromatograms obtained with an equilibrium-dispersive model. Models are useful only insofar as they represent reasonably well what happens in the unit. Computer calculations may then be used to improve on the design and to optimize the experimental conditions for maximum production rate or, more often, for minimum specific production cost. Before any extensive use of a model can be contemplated, however, its validation is required.

The goal of this article is to compare the experimental performance of an SMB with the results of model calculations. In this preliminary work, we have operated our SMB under linear conditions. The design of the system allows the simultaneous recording of the concentration profiles eluted from one column during each successive period as well as that of the concentration histories at the extract and raffinate ports. These profiles are compared to the results given by the exact analytical solution of the ideal model (Zhong and Guiochon, 1996) and by the numerical solution of the equilibrium-dispersive model described previously (Yun et al., 1996).

Theory

The models used in this work have been discussed previously (Yun et al., 1996; Zhong and Guiochon, 1996). Here we give only a brief description.

Column models

Ideal Model. In the ideal model, the column efficiency is supposed to be infinite. The local concentration in the solid phase is related to the liquid-phase concentration through the isotherm, which is linear in the present case. The axial dispersion coefficient is zero. The differential mass balance in column j, for component i, is written

$$\frac{\partial C_{i,j}}{\partial t} + u_j \frac{\partial C_{i,j}}{\partial z} + F \frac{\partial q_{i,j}}{\partial t} = 0, \tag{1a}$$

where $C_{i,j}$ and $q_{i,j}$ are the liquid- and solid-phase concentrations of component i in column j, respectively; u_j is the liquid-phase velocity in column j; $F = (1 - \epsilon)/\epsilon$ is the phase ratio; and ϵ is the total column porosity. Since we consider the separation of a binary mixture and a four-column SMB system, $i = 1, 2$ and $j =$ I, II, III, or IV.

The solution of the ideal model is characterized by the association of a migration velocity with each concentration (Rhee et al., 1989; Guiochon et al., 1994). In the case of a linear isotherm, this velocity is constant. Concentration discontinuities of the boundary condition are unchanged and propagate without dispersion. In the case of a linear isotherm, the solution of the ideal model is trivial with the boundary conditions of elution chromatography. It is easily shown that the injection pulse of each feed component is merely transported along the column at constant velocity, without experiencing any profile change. In the case of SMB, because the boundary conditions are more complex, the solution is also more complex. It conveys much useful information regarding the behavior of the SMB, the concentration profiles along the columns, and at the drawoff ports. This exact analytical solution was discussed previously (Zhong and Guiochon, 1996).

Equilibrium-Dispersive Model. The equilibrium-dispersive model is nonideal. It still assumes constant equilibrium between the two phases, but accounts for the dispersive effect of a finite column efficiency by using an appropriate apparent axial dispersion coefficient, D_a (Guiochon et al., 1994). The mass-balance equation is written

$$\frac{\partial C_{i,j}}{\partial t} + u_j \frac{\partial C_{i,j}}{\partial z} + F \frac{\partial q_{i,j}}{\partial t} = D_a \frac{\partial^2 C_{i,j}}{\partial z^2}. \tag{1b}$$

In both models, the mass-balance equation must be completed by the isotherm equation. In the present case, the equilibrium isotherm is considered to be linear; hence,

$$q_{i,j} = f_{i,j}(C_{1,j}, C_{2,j}) = K_i C_{i,j}. \tag{2}$$

With a linear isotherm, there is no competition between the feed components for interaction with the solid phase. Component 1 is assumed to be less retained than component 2, that is, $K_1 < K_2$.

Initial and Boundary Conditions. At the beginning of the first period of startup, the solid and liquid phases are in equilibrium in the column, with no feed components. Then, a stream of feed is pumped into the column. The initial and boundary conditions of the problem are

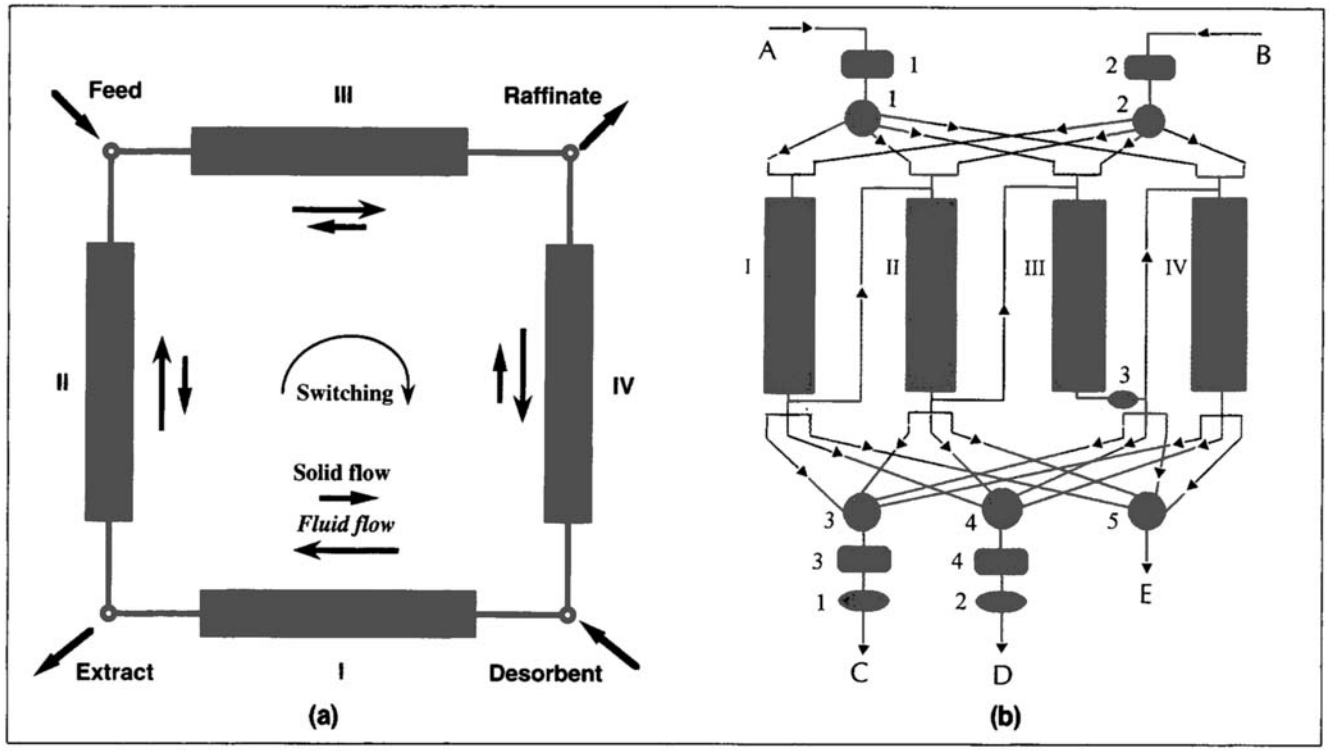

Figure 1. Simulated moving bed separations.

(a) Scheme of the SMB; (b) SMB chromatograph setup. *Rectangles:* columns (or multicolumn sections) I, II, III, IV. *Circles:* 1 feed valve; 2 solvent valve; 3 raffinate valve; 4 extract valve; 5 recycle valve. *Rounded Rectangles:* 1 feed pump; 2 solvent pump; 3 raffinate pump; 4 extract pump. *Ellipses:* 1 raffinate detector; 2 extract detector; 3 on-column detector (detector 3). A: from feed reservoir; B: from mobile phase reservoir; C: to raffinate collector; D: to extract collector; E: to recycle reservoir.

$$C_{i,j}(x,0) = 0, \qquad q_{i,j}(x,0) = 0 \tag{3a}$$

$$C_{i,j}(0,t) = C_{i,j}^{in}, \qquad q_{i,j}(0,t) = f_i\left(C_{1,j}^{in}, C_{2,j}^{in}\right), \tag{3b}$$

where $C_{i,j}^{in}$ is the concentration of component i in the liquid phase at the inlet of column j.

In SMB, the feed and drawoff nodes are shifted after a certain time or cycle time, t^*, to the next position along the fluid-flow direction. This creates an apparent or simulated countercurrent motion of the solid phase, as shown in Figure 1a. Accordingly, after the end of each period, the initial and boundary conditions must be updated. This is done by using the node conditions (see below). The initial concentration profile of component i in column j is the concentration profile in column $j+1$ at the end of the previous period. The composition of the stream entering column j is derived from that of the stream leaving column $j-1$, modified by the node conditions. Note that this model does not consider the extra-column mixing and dispersion that takes place in the connecting tubes, valves, and pumps.

Node model

The equations giving the flow balance and the integral mass balance of each component at each node were derived by Ruthven and Ching (1989). In these equations, Q_{I}, Q_{II}, Q_{III}, Q_{IV} are the flow rates through the corresponding columns; Q_D is the desorbent flow rate; Q_E, the extract flow rate; Q_F, the feed flow rate; and Q_R, the raffinate flow rate. There is a set of equations at each node.

Desorbent node (eluent):

$$Q_{\mathrm{IV}} + Q_D = Q_{\mathrm{I}}$$

$$C_{i,\mathrm{IV}}^{ou} Q_{\mathrm{IV}} + C_{i,D} Q_D = C_{i,\mathrm{I}}^{in} Q_{\mathrm{I}}. \tag{4a}$$

Extract drawoff node:

$$Q_{\mathrm{I}} - Q_E = Q_{\mathrm{II}}$$

$$C_{i,\mathrm{I}}^{ou} = C_{i,\mathrm{II}}^{in} = C_{i,E}. \tag{4b}$$

Feed node:

$$Q_{\mathrm{II}} + Q_F = Q_{\mathrm{III}}$$

$$C_{i,\mathrm{II}}^{ou} Q_{\mathrm{II}} + C_{i,F} Q_F = C_{i,\mathrm{III}}^{in} Q_{\mathrm{III}}. \tag{4c}$$

Raffinate drawoff node:

$$Q_{\mathrm{III}} - Q_R = Q_{\mathrm{IV}}$$

$$C_{i,\mathrm{III}}^{ou} = C_{i,\mathrm{IV}}^{in} = C_{i,R}. \tag{4d}$$

In these equations, $C_{i,j}^{ou}$ and $C_{i,j}^{in}$ are the concentrations of components i at the outlet and the inlet of column j, respectively. Q_j is the flow rate through column j. It is related to the liquid-phase velocity, u_j, by $Q_j = \epsilon A u_j$, where A is the column cross-section area, which is assumed to be the same for all the columns.

Estimation of the Flow Rates and of the Switching Time. Some relationships must be satisfied in each column in order that the lesser retained component moves in the direction of the liquid phase and the more retained one in the direction of the solid phase. These relationships can be reduced to only four because in columns I and III the more strongly adsorbed component is the critical component, while in columns II and IV it is the less adsorbed component that is the critical one. If we assume with Ruthven and Ching (1989) that the four critical flow constraints are all satisfied by the same margin, $\beta(>1)$ (i.e., with the same safety coefficient in all four columns), we obtain the following equations:

$$\frac{Q_I}{Q_S} = K_2\beta + \frac{1}{F} \tag{5a}$$

$$\frac{(Q_I - Q_E)}{Q_S} = K_1\beta + \frac{1}{F} \tag{5b}$$

$$\frac{(Q_I - Q_E + Q_F)}{Q_S} = \frac{K_2}{\beta} + \frac{1}{F} \tag{5c}$$

$$\frac{(Q_I - Q_E + Q_F - Q_R)}{Q_S} = \frac{K_1}{\beta} + \frac{1}{F}. \tag{5d}$$

The optimum design for maximum purity of an SMB would correspond to the limit value, $\beta = 1$, for the production of extract, and $\beta = \sqrt{\alpha}$ for the production of raffinate. In practice, it is impossible to operate the SMB with either value. β is usually chosen to be slightly larger than 1, which introduces a safety margin.

The system of algebraic linear equations (Eqs. 5a–5d) can be easily solved by eliminating Q_I:

$$Q_S = \frac{Q_F}{K_2/\beta - K_1\beta} \tag{6a}$$

$$Q_E = Q_S(K_2 - K_1)\beta = \frac{Q_F(K_2 - K_1)\beta}{K_2/\beta - K_1\beta} \tag{6b}$$

$$Q_R = Q_S(K_2 - K_1)/\beta = \frac{Q_F(K_2 - K_1)/\beta}{K_2/\beta - K_1\beta}. \tag{6c}$$

Knowing the solid-phase flow rate, Q_S, we can derive the value of the switching time, t^*, in an SMB system equivalent to a given moving bed (TMB). It is given by

$$t^* = \frac{L}{u_s} = \frac{(1-\epsilon)LA}{Q_S}. \tag{7}$$

It is obvious that we must have $\beta < \sqrt{K_2/K_1} = \sqrt{\alpha}$ to achieve positive values of all the flow rates. This result demonstrates why it is difficult to separate two closely eluted components (i.e., a pair such that $K_2/K_1 = \alpha$ is close to 1) in SMB. The closer α is to 1, the less flexibility there is for the choice of β.

All the flow rates can be calculated using Eqs. 4, 5 and 6 from the feed flow rate and the margin, β.

Table 1. Characteristics of the Columns Used

Column	t_0 (min)	F	K_1	K_2	α	N_1	N_2	N_2/N_1
A	2.190	0.7565	1.386	2.326	1.678	2,304	2,271	1.015
B	2.202	0.7468	1.401	2.388	1.704	2,856	2,820	1.013
C	2.194	0.7532	1.403	2.376	1.694	3,653	3,406	1.073
D	2.194	0.7532	1.405	2.362	1.687	1,742	1,756	0.992
E	2.189	0.7572	1.400	2.354	1.681	3,810	3,610	1.055
F	2.190	0.7565	1.424	2.405	1.689	2,006	2,049	0.979
G	2.201	0.7476	1.400	2.380	1.700	3,739	3,643	1.026
H	2.192	0.7549	1.351	2.283	1.690	4,261	4,181	1.019
Avg.	2.194	0.7532	1.397	2.359	1.690	3,046	2,967	1.021
RSD (%)	0.22	0.53	1.51	2.96	0.52	31	29.5	3

Flow rate, 2 mL/min; component 1: 2-phenylpropanol; component 2: 3-phenyl-1-propanol.

Experiment

Columns and chemicals

Eight columns (1.0 cm × 9.8 cm) were slurry packed in-house at 6,000 psi (41 MPa) with 10 μm Zorbax spherical C-18 bonded silica, with an average pore size of 150 Å (BTR, Wilmington, DE) column. The packing procedure was previously described, as were the problems encountered in packing columns with highly reproducible performance (Stanley et al., 1996). The parameters of the eight columns are listed in Table 1. Columns A to D were used in the experiments made with four columns (one column per SMB section), and columns A to H in the experiments made with eight columns (two columns per SMB section). Note that the column-to-column fluctuations of the holdup time, phase ratio, and retention factor have all a relative standard deviation (RSD) of 0.5 % or lower. The RSD of two retention factors of the two components are larger; they are approximately proportional to the retention factor which, together with the small RSD of the holdup time, suggests that these fluctuations are due to fluctuations of the amount of surface area of adsorbent available in each column. Finally, the column efficiency is much less reproducible than any of the other column parameters. Note, however, that the fluctuations of the ratio of the efficiencies of the two components are much smaller, with an RSD of 3%, comparable to the one observed on the second retention factor.

2-Phenyl ethanol and 3-phenyl-1-propanol were purchased from Fluka (Ronkonkoma, NY). 2-Phenyl ethanol is the lesser retained component, with $k_1 = 1.397$. 3-phenyl-1-propanol is the more retained component, with $k_2 = 2.359$. The resulting value of the separation factor, $\alpha = 1.69$, together with data in the literature suggest that the separation of these two components should not be a difficult one to perform with an SMB.

The mobile phase was a 60:40 methanol/water solution. All concentrations are reported in mg/mL. A concentration of 1 mg/mL is 8.2 mM for 2-phenyl ethanol and 7.4 mM for 3-phenyl-propanol. Methanol and water are purchased from Burdick and Jackson (Muskegon, MI). All products were used without further purification. Different feed compositions were used for the study of the four-column than for the eight-column SMBs (see figure captions).

Analytical chromatography

All experiments involving conventioned liquid analytical chromatography were performed on a Gilson system (Mid-

dleton, WI), which consists of three Model 302 pumps, a 6-port Valco (Houston, TX) electrically actuated valve fitted a 0.02-mL sample loop. The effluent composition was monitored by a Spectroflow 757 variable-wavelength UV detector (Applied Biosystems, Ramsey, NJ) at 265 nm. The columns were tested with this system.

SMB chromatography

The SMB chromatography is a Laboratory Scale Continuous Chromatography system, model ICLC 16-10, from Prochrom (Indianapolis, IN; Champigneulles, France). The system consists of four HP1050 pumps (Hewlett-Packard, Palo Alto, CA), one feed pump, one solvent (liquid-phase) pump, one raffinate pump, and one extract pump. Five electropneumatic 16-port valves are controlled by a computer to actuate the SMB. One valve is connected to the feed port, one to the solvent port, one to the raffinate port, one to the extract port, and the last one to the recycle port. The equipment can be operated at a maximum inlet pressure of 70 atm. It is able to run with 8, 12, or 16 columns, with any number of columns in each of the four sections (provided the total number of columns is 8, 12, or 16). For the experiments made with four columns, we used the eight-column setup and replaced the first column of each section by a 31-cm-long, 0.05-cm-i.d. stainless-steel tubing.

The flow rate delivered by each pump and the movement of each valve are controlled by the CHROSOFT software (CHROSOFT Manual, Prochrom, Champigneulles, France, 1996). Figure 1b shows the flow sheet of the system. Although four columns are drawn on the figure, a setup with more columns can be easily done with slight modifications of the tubing connections.

Detection

Three UV spectrophotometric detectors, all operating at 265 nm, were connected to the SMB for the purpose of this study, as shown in Figure 1b, although only one (preferably two) would be needed in production runs. The first two detectors (both Spectroflow 757, variable-wavelength UV detectors, Applied Biosystems, Ramsey, NJ) were located on the extract line, between the extract pump and the extract collector, and on the raffinate line, between the raffinate pump and the raffinate collector, respectively. They monitor the concentration histories at these two ports. The third detector (HP1100, variable-wavelength UV detector, Hewlett-Packard, Palo Alto, CA) was equipped with a high-pressure flow cell, which could be connected on the main stream of the SMB, between the end of one column section and one of the rotary valves. The signal recorded with this detector is related to the concentrations of the two components eluting from the column. If the detector response is linear, it is equal to $S_1C_1 + S_2C_2$, S_i being the response factor of component i. In general, the UV spectra of the two feed components are too close, the detector cannot distinguish between them, and their separate quantitation is not possible. Conversely, however, knowing the concentration profiles of the two components along the series of columns in the SMB and the response factors of the detector allows us to calculate these elution profiles for any position of the detector in the SMB. Thus, this arrangement allows an independent test of the validity of the concentration profiles calculated from numerical solutions of the models and permits an instructive comparison between experimental and numerical results.

Care was taken to use concentrations low enough to achieve both linear-isotherm behavior of both components and a linear response of all three detectors. In this particular case, the concentration required to achieve a linear-detector response is lower than the concentration required for linear-isotherm behavior. The response factors for the two compounds used are slightly different. Calibrations of the detectors at 265 nm gave slopes of 1.87 and 1.56 for the plots of the UV absorbance (in mAu) vs. the concentration (in mg/mL) of the solution in the detector cell, respectively, for 2-phenyl ethanol and 3-phenyl-1-propanol. The mobile-phase flow rate has no influence on these response factors, but changes in flow rate result in a base-line shift. A correction is required. The concentration profiles of the two compounds in the four-column SMB overlap in the whole section III of the SMB (at the end of a period) and in the end of column II and the beginning of column IV. In this important mixed zone, it is impossible to distinguish the contributions of each component to the overall detector response. To compare experimental and calculated profiles, we convert the calculated concentration profiles into detector response by summing the products of the response factor and the concentration for each compound. This gives a calculated response curve for the third detector.

Results and Discussion

The concentration of all the feed samples used was low enough to ensure that both the isotherm and the detector response were linear, as explained earlier. The β value was chosen as 1.15 (intermediate between 1 and $\sqrt{\alpha} = 1.30$). From this value and knowing the phase ratio and the retention factors of the two components, all the flow rates and the switching time were determined as described in the Theory section. The pertinent values are given in the figure captions. The responses of the three detectors were recorded under these experimental conditions. The numerical solutions of the ideal and equilibrium-dispersive models were also calculated under these conditions. The results obtained are compared in the following figures.

The variation of the composition of the eluent as a function of time can be studied in two different ways. First, it can be described from the point of view of the detectors that are located on the extract and raffinate lines, downstream of the corresponding rotary valves. If there is no back mixing between the column exit and the detector cell, the detector response will show an oscillation of the concentration during each period, with a progressive increase in the average concentration during each cycle as the startup of the unit progresses and the system tends toward steady state. The resolution between the concentration peaks eluted during each period depends on the column efficiency. With low-efficiency columns, it may not be noticed (see below). The second way to study the variations of the composition of the liquid phase as a function of time consists of monitoring the signal of a detector fixed at the end of one column. Then the position of the detector cell in the SMB scheme moves along with that of the column in the train at the end of each successive period. Thus, it is located successively at each of the connecting points

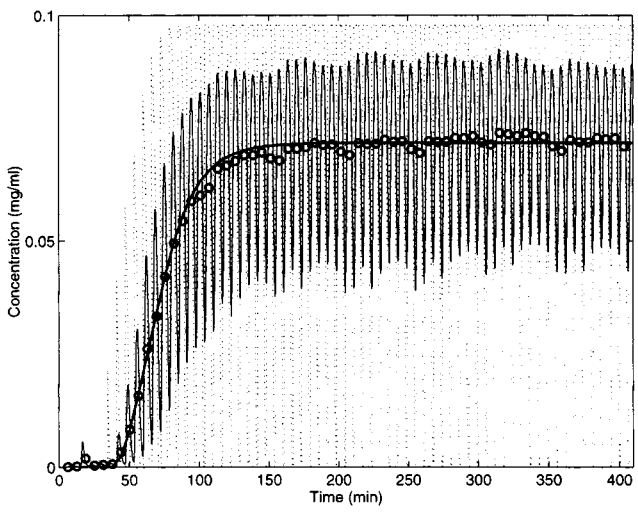

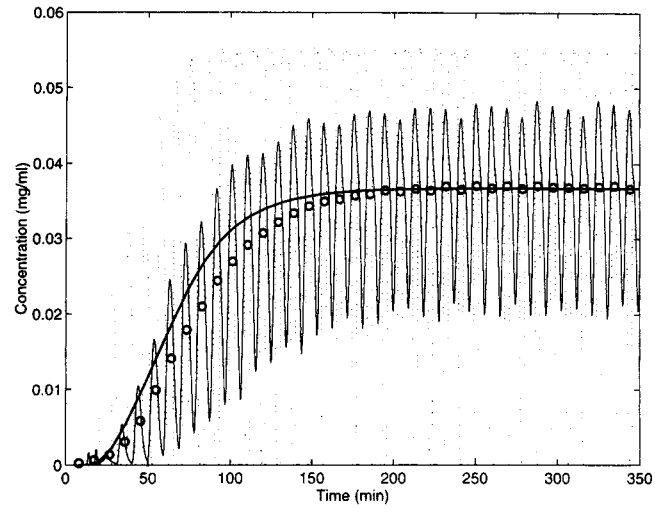

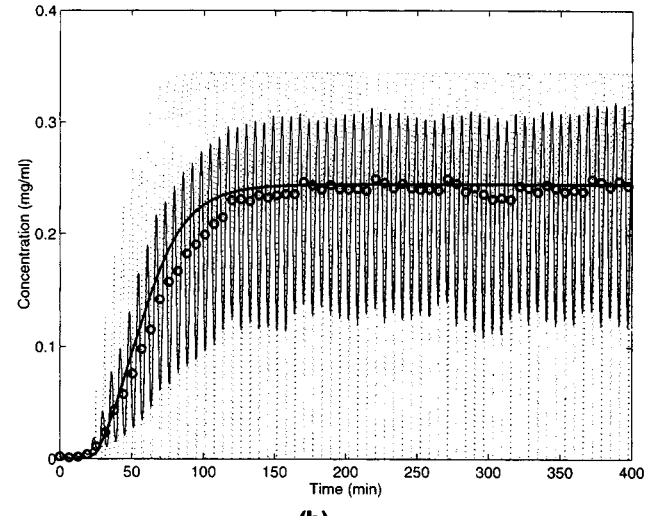

Figure 2. History of concentrations at the draw-off nodes

(a) History of the extract concentrations for an eight-column SMB. *Thin sold line:* recorded concentration profile. *Dotted line:* calculated concentration profile. *Circles:* experimental data, concentration averaged over one cycle. *Thick solid line:* calculated concentration averaged over one cycle. *Experimental conditions*: average isotherm coefficients, $k_1 = 1.3987$, $k_2 = 2.3936$; safety factor, $\beta = 1.12$; column porosity, $\epsilon = 0.5690$; cycle time, $t^* = 6.3086$ min. *Column flow rates:* $Q_I = 2.1039$ mL/min; $Q_{II} = 1.5180$ mL/min; $Q_{III} = 1.8180$ mL/min; $Q_{VI} = 1.3509$ mL/min. *Feed concentrations*: 0.1118 mg/mL of 2-phenylethanol, and 0.5635 mg/mL of 3-phenyl-propanol. (b) History of the raffinate concentrations for an eight-column SMB. Same conditions and symbols as in Figure 2a. (c) History of the extract concentrations for a four-column SMB. Same symbols as in Figure 2a. *Experimental conditions:* average isotherm coefficients; $a_1 = 1.4028$, $a_2 = 2.3762$; safety factor, $\beta = 1.15$; column porosity, $\epsilon = 0.5717$; cycle time, $t^* = 9.33$ min. *Column flow rates:* $Q_I = 1.4365$ mL/min; $Q_{II} = 1.0412$ mL/min; $Q_{III} = 1.2012$ mL/min; $Q_{VI} = 0.9022$ mL/min. *Feed concentrations:* 0.1152 mg/mL of 2-phenylethanol, and 0.0908 mg/mL of 3-phenyl-propanol.

between two columns in the train (Figure 1a), for example, between sections II and III, or in the middle of section II between its two columns (if there are two columns per SMB section), or between sections I and II. It returns to the same position after a number of cycles equal to the number of columns in the unit (later called the superperiod). Note that when the valve position changes, the velocity of the solute will change if the column is shifted from one section of the SMB to another, because the flow rate is different in each section. This causes no changes in the response factors, just a base-line shift for detector #3, which was accounted for in all calculations. During each successive period, this detector gives the profile of UV absorbance of the eluent moving from one column to the next, through the cell of this detector. When a pure compound is eluted, either as raffinate or as extract, it would be easy to convert the detector signal into the actual concentration profile along the column located upstream, using the response factor of the detector and the conventional relationship between retention times at the end of the column and positions in this column at the beginning of the period. In linear chromatography this relation is simple. The position, x, of a concentration at the beginning of the period is related to its elution time (measured from the beginning of the period), t, by $x = v_i t$, where v_i is the linear velocity of the solute ($v_i = u/(1 + Fk_i)$) along the column (NB: This velocity changes every time the column moves into a different section of the SMB). However, it is impossible to derive the individual elution profiles of the two components from the profile of UV absorbance during the elution of the mixed band contained in the central columns of the SMB. The UV spectra of these compounds are too similar. On the other hand, the UV absorbance profile of any column is easy to derive from the individual band profiles. So, comparisons will be made later between calculated and experimental profiles of the UV absorbance at the exit of each column. Note that for better clarity this comparison is made under steady state.

Figures 2a to 2c illustrate the concentration histories at the product ports of the SMB. Figure 2a shows the history of the extract concentrations, and Figure 2b shows the history of

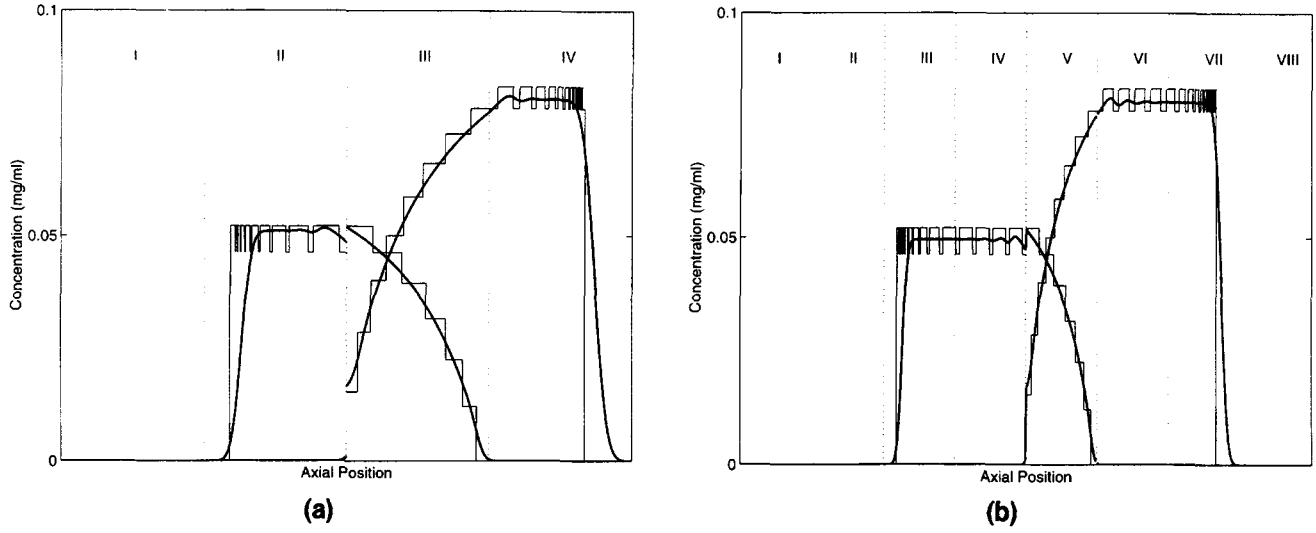

Figure 3. Band profiles along the columns of an SMB calculated using the ideal model (thin solid lines) and the equilibrium-dispersive model (thick solid lines).

(a) Four-column SMB. Same experimental conditions as in Figure 2c. (b) Eight-column SMB. Same experimental conditions as in Figure 2a.

the raffinate concentrations for an eight-columns SMB. For the sake of comparison, Figure 2c shows the history of the extract concentrations for a four-column SMB. Note that the resolution observed in the experimental records (thin solid lines) is somewhat less than the one predicted by the equilibrium-dispersive model (dotted lines). This is explained by the significant amount of band spreading in the rotary valve, the long connecting tubes, and the pump, which are on both the extract and the raffinate lines of the SMB. The pump operates as an ideal mixer, completely homogenizing the content of the pump cylinder during each pump cycle. The calculations were made by introducing the values of the efficiency in Table 1, measured on each column, into the program. This definitively overestimates the total column efficiency and, accordingly the degree of resolution between the successive peaks of 2-phenyl ethanol (at the raffinate port; Figure 2b) and 3-phenyl-1-propanol (at the extract port; Figure 2a). Note that, by contrast, there is excellent agreement between the average value of the stream composition calculated from the equilibrium-dispersive model (thick solid lines) and the detector response. This permits another comparison between the model of SMB and experimental results. For the sake of clarity, Figure 3 shows the steady-state band profiles along the columns of the four-column (Figure 3a) and the eight-column (Figure 3b) SMB, calculated from the ideal model and from the equilibrium-dispersive model. Obviously, during the startup period, this method gives concentration profiles that are more difficult to interpret because they correspond to successive periods, not to the same one. The profiles shown in the following figures were all obtained under steady-state conditions.

Figures 4 and 5 compare the experimental response profiles of the third detector and the value calculated from the individual concentration profiles and the response factors, as explained earlier. There is an excellent agreement between the calculated profile (solid lines) and the experimental result (symbols), for a four-column SMB (Figure 4) as well as for an eight-column SMB (Figure 5). To explain these figures, we must note first that we have two configurations that rotate relative to each other by $1/n$ (n = number of columns) turn at each period. There is a physical configuration made of n columns, numbered A to D ($n = 4$) or A to H ($n = 8$) connected to five rotary valves in such a way that a solution moves from one column to the other in alphabetical order. This column order is never altered. Then we have a process order that also remains constant and that is related to the relative position of the four streams of the equipment. In the case for which $n = 8$, for example, positions I.1 and I.2 are located between the desorbent inlet and the extract outlet; positions II.1 and II.2 are located between the extract outlet and the feed inlet; positions III.1 and III.2 between the feed inlet and the raffinate outlet; and positions IV.1 and IV.2 between the raffinate outlet and the desorbent inlet. Any given column, for example, D, successively takes the different positions in the order IV.2, IV.1, III.2, ... II.1, I.2, and I.1, to return at I.1, and so forth indefinitely. Figures 4 and 5 present a series of, respectively, four and eight juxtaposed panels that show the successive records of the detector-3 signal during as many consecutive periods of operation of the SMB. Table 2 lists the correspondences between the panels and successive positions of the column upstream from detector 3 in the SMB scheme (Figure 1a).

There are four juxtaposed panels in Figure 4a. The first panel shows the history of the eluent concentration when the column immediately upstream from detector 3 is in position IV. Nothing exits from the column, which is in agreement with the independent observation that there is no 2-phenyl ethanol in the raffinate (which is collected between sections III and IV) nor in the liquid phase recycled from the exit of column IV to the inlet of column I and which was sampled (Figure 6a). The second panel gives the concentration history at the outlet of the column when it is in position III. During that time, 2-phenylethanol breaks through column III to enter column IV through detector 3. This compound is practically pure, as confirmed by the analysis of the raffinate (Figure 6a). The third panel shows the concentration history at

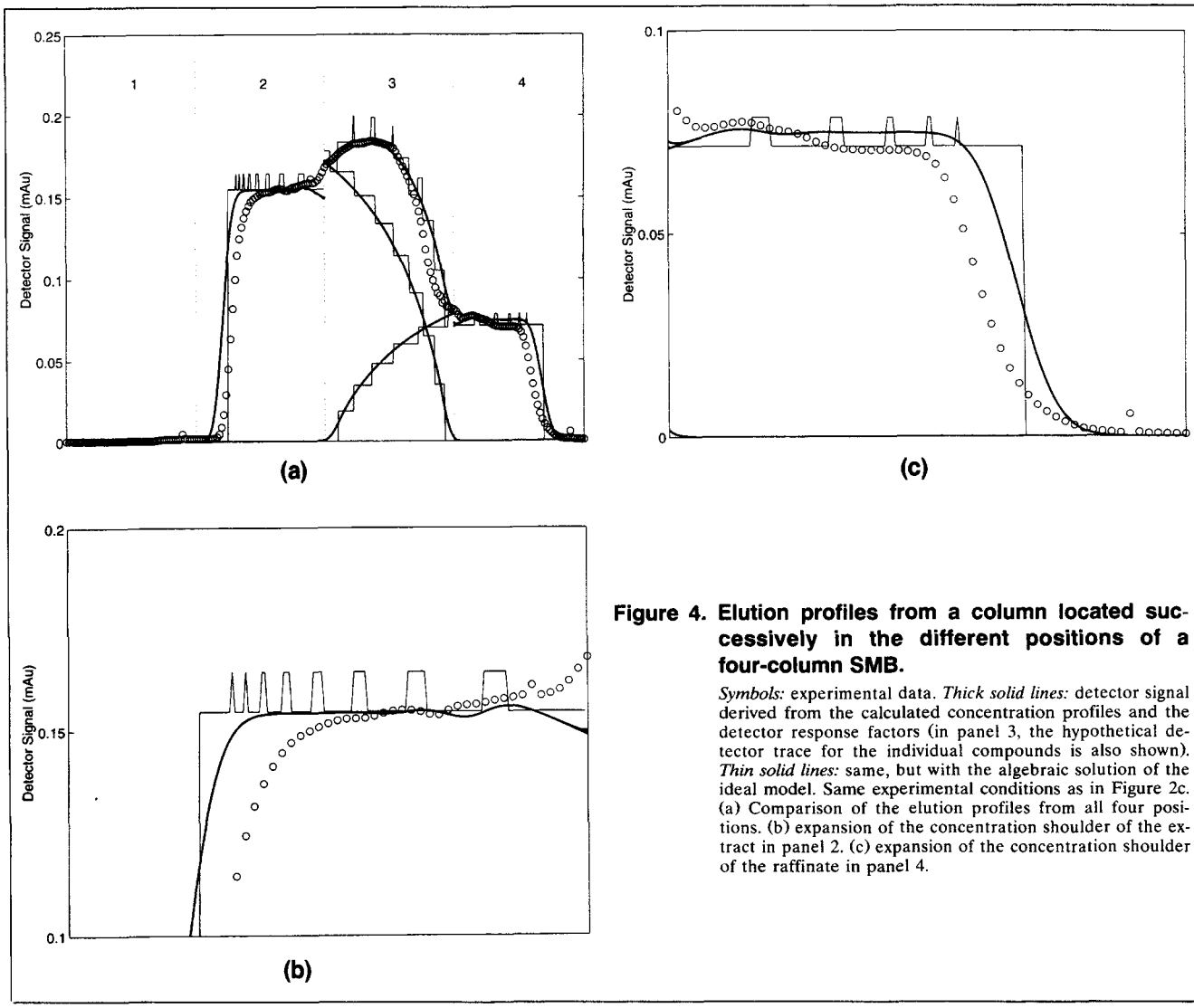

Figure 4. Elution profiles from a column located successively in the different positions of a four-column SMB.

Symbols: experimental data. *Thick solid lines:* detector signal derived from the calculated concentration profiles and the detector response factors (in panel 3, the hypothetical detector trace for the individual compounds is also shown). *Thin solid lines:* same, but with the algebraic solution of the ideal model. Same experimental conditions as in Figure 2c. (a) Comparison of the elution profiles from all four positions. (b) expansion of the concentration shoulder of the extract in panel 2. (c) expansion of the concentration shoulder of the raffinate in panel 4.

the exit of the column when it is in section II. This column contains a mixed band, which explains the round top of the absorbance profile, which results from the simultaneous rise of the concentration of 3-phenyl-1-propanol and decay of the concentration of 2-phenylethanol. Also in this panel are shown the concentration profiles of the two components, for the sake of comparison. Finally, the fourth panel corresponds to the concentration profile recorded at the exit of the column when positioned in section I. The eluted band contains practically only 3-phenyl-1-propanol, as confirmed by analysis of the extract stream, which contains only very small amounts of 2-phenylethanol (Figure 6a). The agreement between the experimental and the calculated profiles is excellent. Note that the experimental profiles include the slight oscillations on the plateaus of the concentration profiles eluted from sections I and III that are the result of the dispersion of the concentrations oscillations predicted by the ideal model (Zhong and Guiochon, 1996). The thin solid line in Figure 3a was derived from the exact algebraic solution of the ideal model for a four-column SMB (Zhong and Guiochon, 1996), in the same way as described earlier for the conversion of the solution of the equilibrium-dispersive model into a UV absorbance elution profile. Figures 4b and 4c provide enlargements of the results in panels 2 and 4, respectively. There is also an excellent agreement between the calculated and the experimental profiles. The slight oscillations seen on the two plateaus correspond to the dispersion of the square-wave pattern predicted by the ideal model. These oscillations were not reported before. Clearly, these oscillations are real, resulting from the periodic nature of the SMB, and are not caused by a numerical instability in the calculation of solutions of the equilibrium-dispersive model.

A similar result is shown in Figure 5a, which compares the calculated and experimental histories of eluent concentrations at the exit of the column in its eight successive positions, in the case of an eight-column SMB. There are now eight panels in the figure, corresponding to the eight successive possible positions of the column whose effluent is monitored by detector 3. The first and the last panel are empty. They correspond, respectively, to positions 8 and 1 of the column (i.e., as columns I.1 and IV.2, respectively). We have shown elsewhere (Zhong et al., in preparation) that, under

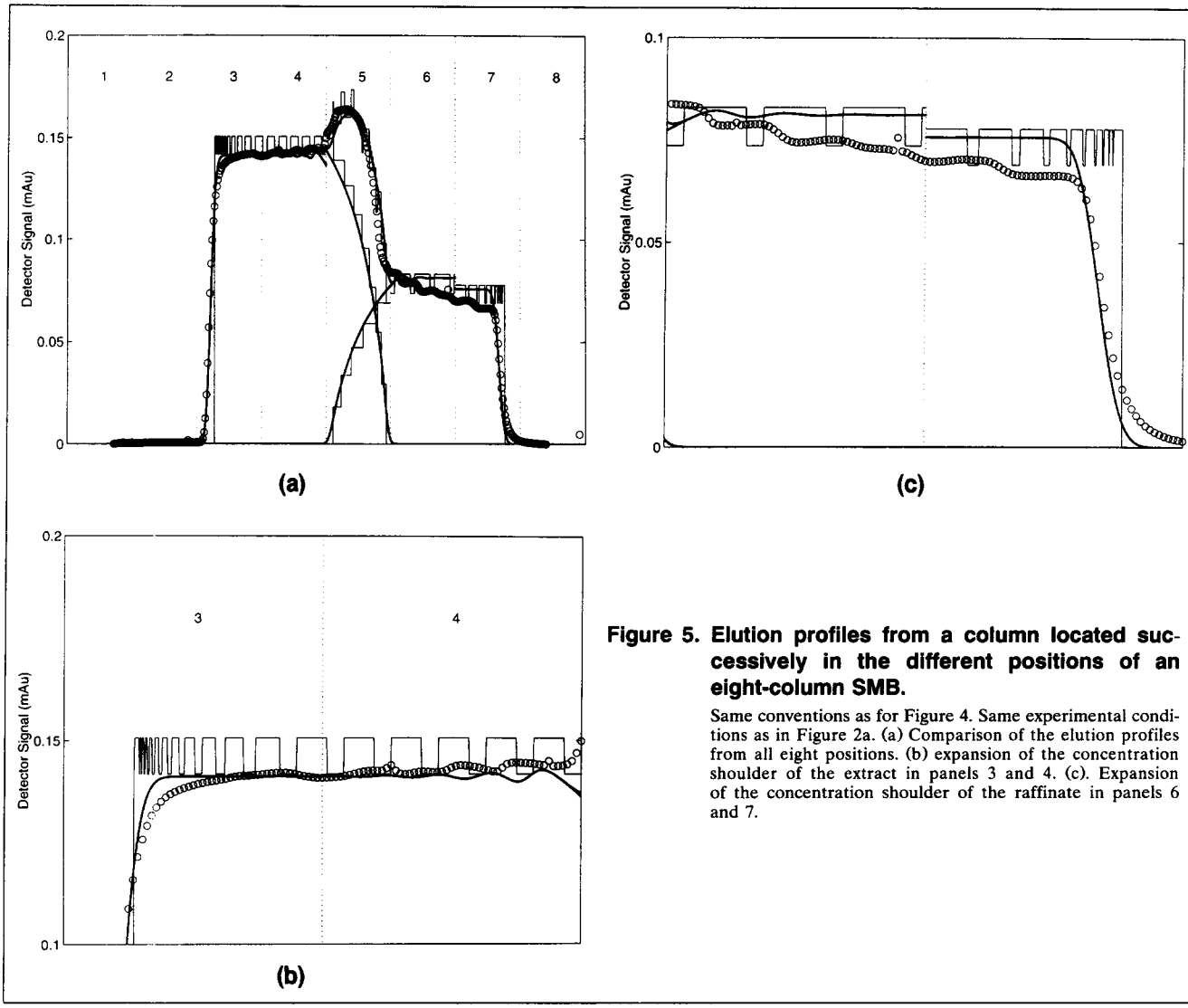

Figure 5. Elution profiles from a column located successively in the different positions of an eight-column SMB.

Same conventions as for Figure 4. Same experimental conditions as in Figure 2a. (a) Comparison of the elution profiles from all eight positions. (b) expansion of the concentration shoulder of the extract in panels 3 and 4. (c). Expansion of the concentration shoulder of the raffinate in panels 6 and 7.

the conventional conditions of SMB operation, the first component cannot penetrate into column IV.2 unless the column efficiency is very poor and the front of the profile very diffuse, which is not the case with the columns used here. Similarly, except under conditions of extremely strong apparent axial dispersion, the second component is entirely eluted from column I.2 during a period, so it cannot move back and reach into column I.1 at any time. Obviously, in the present case, the SMB could be operated with only six columns, two each in sections II and III, one each in sections I and IV. The same performance would be achieved. That panel 2 (elution profile at the exit of the column in position IV.1) is empty is in agreement with the analysis of samples of the liquid phase recycled through the unit (between sections IV.2 and I.1): no feed component elutes from columns IV.2, the last column of the SMB to be recycled into the first one during the next period. These analyses (Figure 6b) are discussed later. Panel 3 shows the elution profile of the column when in position III.2. The eluent contains pure 2-phenylethanol and no 3-phenyl-1-propanol. This position corresponds to the exit of the raffinate stream, which is split just downstream of detector 3, between the drawoff port and the entrance to column IV.1. The purity of the raffinate stream is confirmed by its analysis (Figure 6b). The fourth panel shows the concentration profile at the exit of the column when it is in position III.1. It shows a peak concentration of 2-phenylethanol. Some weak oscillations can be seen on this peak, in agreement with the calculated profile. They result from the dispersion of the

Table 2. Correspondence between Panels in Figures 4 and 5 and Column Position in the SMB Scheme

Panel No.	Column Position ($N=8$)	Column Position ($N=4$)
1 (I)	I.1	IV
2 (II)	IV.2	III
3 (III)	IV.1	II
4 (IV)	III.2	I
5 (V)	III.1	
6 (VI)	II.2	
7 (VII)	II.1	
8 (VIII)	I.2	

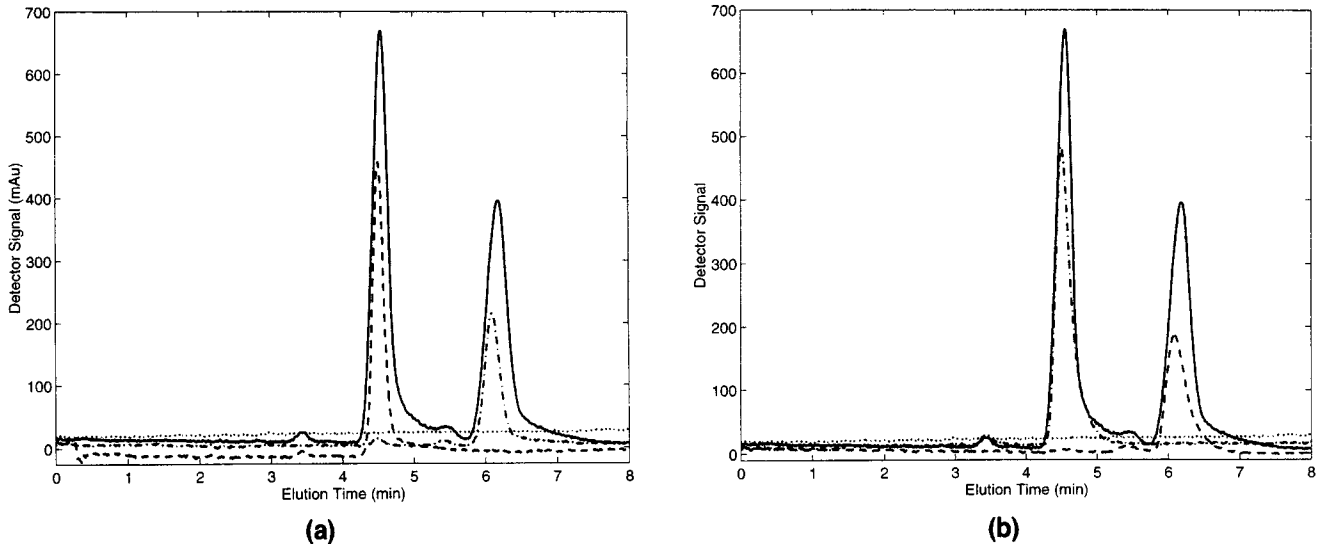

Figure 6. Analytical chromatograms for the feed, the extract, the raffinate, and the recycle fraction of the SMB.

Solid line: feed sample. *Dot-dashed line:* raffinate sample. *Dashed line:* extract sample. *Dotted line:* recycle sample. (a) Case of a four-column SMB. (b) Case of an eight-column SMB.

rectangular pattern of oscillations predicted by the ideal model (see later). The mixed zone is essentially contained in panel 5, which shows the calculated UV absorbance profiles of both components (solid lines), the total absorbance profile (thick solid line), and the experimental profile or history of UV absorbance at the outlet of column II.2 (symbols). The experimental profiles in panels 6 and 7 are the concentration histories recorded by detector 3 when the column upstream of this detector is located in positions II.1 and I.2, respectively. Panels 6 and 7 contain a plateau of nearly pure 3-phenyl-1-propanol (panel 6) and its front (panel 7). This is confirmed by the results of the extract analysis (Figure 6b), which shows no presence of 2-phenylethanol.

Figures 5b and 5c compare the experimental profiles of UV absorbance at the exit of column positions III.2 and III.1, and II.1 and I.2, respectively, with the profiles calculated using the equilibrium-dispersive model and the exact algebraic solution of the ideal model for an eight-column SMB (Zhong and Guiochon, in preparation). These elution profiles are those of pure 2-phenylethanol and 3-phenyl-1-propanol, respectively. As in the case of the four-column SMB, these figures show excellent agreement between the calculated and experimental profiles, with slight oscillations corresponding to the axial dispersion of the square-wave pattern predicted by the ideal model.

In both Figures 4 and 5, there is excellent agreement between the measured and calculated profiles of the UV absorbance at the exit of the column in all four positions (Figure 4), and at the column exit in all eight positions (Figure 5). From this it follows that there must be an excellent agreement between the actual and the calculated concentration profiles along the axes of these four or eight columns. This confirms the conclusions already derived from the concentration histories at the extract and the raffinate ports. The slight differences in Figure 5a between the calculated and observed profiles at the top of the rear front of 2-phenylethanol (panel 3) and at the bottom of the front of 3-phenyl-1-propanol are frequent in this type of comparison (Guiochon et al., 1994). However, we have no explanation for the slight slant of the concentration plateau of 3-phenyl-1-propanol (panels 6 and 7), although we suspect the possibility of a small dead volume in the tubing connections. The excellent separation observed shows that the columns used are much too efficient for the separation required. A higher production rate of 99% pure compounds could be achieved with a lower efficiency. The equipment was designed to separate enantiomers, with a lower separation factor.

Figures 6a and 6b shows the analytical chromatograms obtained for the feed, the extract and the raffinate fractions collected, and the eluent recycled between positions IV and I, respectively, for the four-column SMB, and between positions IV.2 and I.1 for the eight-column SMB. The feed used also contains two minor impurities, one eluted before 2-phenylethanol, and one eluted between the two components. The first impurity was obviously found in the raffinate fraction (dashed line). The second one was found in the extract fraction (dot-dashed line), but could easily have been collected with the raffinate, if needed, by a minor adjustment of the cycle time, that is, of the solid-phase flow rate. Finally, the desorbent recycled to the SMB is pure and contains no detectable amount of either product.

Conclusion

There is complete agreement between the concentration profiles and concentration histories calculated using the equilibrium-dispersive model of chromatography and those measured experimentally, at least under linear conditions. The results shows that it is both possible and tenable to optimize the design and operating conditions of an SMB using computer calculations. These results suggest that fewer columns could be used than has been traditionally accepted. This conclusion must be qualified, however, because the instrument used here was equipped with columns with too high an efficiency. Still, it is highly probable that, in many cases, one fewer column could be used. Finally, this work confirms ex-

perimentally the periodic character of the SMB separator, which is shown by the concentration oscillation on the plateau of the two components. It also indicates that the SMB can be operated with columns that are very similar, but that it may not be necessary to strive too hard to make them identical. This problem will be studied from theoretical and experimental viewpoints.

Acknowledgments

This work was supported in part by Grant CHE-93-01663 from the National Science Foundation and by the cooperative agreement between the University of Tennessee and the Oak Ridge National Laboratory. We acknowledge the support of Maureen S. Smith in solving our computational problems.

Literature Cited

Bailly, M., and D. Tondeur, "Recycle Optimization in Non-linear Productive Chromatography," *Chem. Eng. Sci.*, **37**, 1199 (1982).

Balannec, B., and G. Hotier, "From Batch Elution to Simulated Countercurrent Chromatography," *Preparative and Production Scale Chromatography*, G. Ganetsos and P. E. Barker, eds., Dekker, New York, p. 301 (1993).

Bombaugh, K. J., W. A. Dark, and R. L. Levangie, "High Resolution Steric Chromatography," *J. Chromatog. Sci.*, **7**, 42 (1969).

Broughton, D. B., and C. G. Gerhold, "Continuous Sorption Process Employing Fixed Bed of Sorbent and Moving Inlets and Outlets," U.S. Patent No. 2,985,589 (1961).

Broughton, D. B., "MOLEX, Case History of a Process," *Chem. Eng. Prog.*, **64**, 60 (1968).

Broughton, D. B., R. W. Neuzil, J. W. Pharis, and C. S. Brearley, "The PAREX Process for Recovering Paraxylene," *Chem. Eng. Prog.*, **66**, 70 (1970).

Broughton, D. B., "Adsorptive Separation—Liquids," *Kirk-Othmer Encyclopedia of Chemical Technology*, 3rd ed., Vol. 1, Wiley, New York, p. 563 (1978).

Broughton, D. B., "Production-Scale Adsorptive Separations of Liquid Mixtures by Simulated Moving-Bed Technology," *Sep. Sci. Technol.*, **19**, 723 (1984).

Charton, F., M. Bailly, and G. Guiochon, "Recycling in Preparative Liquid Chromatography," *J. Chromatog. A*, **687**, 13 (1994).

Charton, F., and R.-M. Nicoud, "Complete Design of a Simulated Moving Bed," *J. Chromatog. A*, **702**, 97 (1995).

Ching, C. B., B. G. Lim, E. J. D. Lee, and S. C. Ng, "Preparative Resolution of Praziquantel Enantiomers by Simulated Countercurrent Chromatography," *J. Chromatog.*, **634**, 215 (1993).

DeRosset, A. J., R. W. Neuzil, and D. J. Korous, "Liquid Column Chromatography as a Predictive Tool for Continuous Countercurrent Adsorptive Separations," *Ind. Eng. Chem., Process Res. Dev.*, **15**, 261 (1976).

Fish, B. B., R. W. Carr, and R. Aris, "Design and Performance of a Simulated Countercurrent Moving-bed Separator," *AIChE. J.*, **39**, 1783 (1993).

Guiochon, G., S. G. Shirazi, and A. M. Katti, *Fundamentals of Preparative and Nonlinear Chromatography*, Academic Press, Boston (1994).

Hashimoto, K., Y. Shirai, and S. Adachi, "Models for the Separation of Glucose Fructose Mixtures Using a SMB Adsorber," *J. Chem. Eng. Japan*, **26**, 52 (1993).

Henry, R. A., S. H. Byrne, and D. R. Hudson, "High Speed Chromatography Using an Alternate Pumping Principle," *J. Chromatog. Sci.*, **12**, 197 (1974).

Küsters, E., G. Gerber, and F. D. Antia, "Enantioseparation of a Chiral Epoxide by Simulated Moving Bed Chromatography Using Chiralcel OD," *Chromatographia*, **40**, 387 (1995).

Martin, M., F. Verillon, C. Eon, and G. Guiochon, "Theoretical and Experimental Study of Recycling in High Performance Liquid Chromatography," *J. Chromatog.*, **125**, 17 (1976).

Negawa, M., and F. Shoji, "Optical Resolution by Simulated Moving-bed Adsorption Technology," *J. Chromatog.*, **590**, 113 (1992).

Neuzil, R. W., and R. H. Jensen, "Development of the Sarex Process for the Separation of Saccharides," AIChE Meeting, Philadelphia (1978).

Rhee, H.-K., R. Aris, and N. R. Amundson, "On the Theory of Multicomponent Chromatography," *Proc. R. Soc.*, **A267**, 419 (1970).

Ruthven, D. M., and C. B. Ching, "Counter-current and Simulated Moving Bed Adsorption Separation Processes," *Chem. Eng. Sci.*, **44**, 1011 (1989).

Seidel-Morgenstern, A., and G. Guiochon, "Theoretical Study of Recycling in Preparative Chromatography," *AIChE J.*, **39**, 809 (1993).

Seidel-Morgenstern, A., and G. Guiochon, "Theoretical Study of Recycling in Preparative Chromatography," *AIChE J.*, **39**, 809 (1993).

Seidel-Morgenstern, A., "There is More than Elution in Preparative Chromatography," *Proc. GIT Special Chromatography International*, Git Verlag GmbH, Darmstadt, Germany, p. 32 (1996).

Stanley, B. J., C. R. Foster, and G. Guiochon, "On the Reproducibility of Column Efficiency in High Performance Liquid Chromatography and the Role of the Packing Density," *J. Chromatog. A*, 761, in press (1997).

Storti, G., M. Mazotti, M. Morbidelli, and S. Carra, "Robust Design of Binary Countercurrent Adsorption Separation Processes," *AIChE J.*, **39**, 471 (1993).

Storti, G., M. Masi, S. Carra, and M. Morbidelli, "Optimal Design of Multicomponent Countercurrent Adsorption Separation Processes Involving Nonlinear Equilibria," *Chem. Eng. Sci.*, **44**, 1329 (1989).

Yun, T., Z. Bensetiti, G. Zhong, and G. Guiochon, "Effect of the Column Efficiency on the Internal Concentration Profiles and the Performance of a Simulated Moving Bed Unit in the Case of a Linear Isotherm," *J. Chromatog. A*, **760**, 3 (1997).

Zhong, G., and G. Guiochon, "Analytical Solution for the Linear Ideal Model of Simulated Moving Bed Chromatography," *Chem. Eng. Sci.*, **51**, 4307 (1996).

Zhong, G., T. Yun, P. Sajonz, and G. Guiochon, "Simulated Moving Bed Chromatography. Effect of Column Subdivision in the Linear, Ideal Case," *AIChE J.*, in press (1997).

Manuscript received Oct. 7, 1996, and revision received Dec. 2, 1996.